Article

Not peer-reviewed version

Root Dentine Thickness of Maxillary First Molars in a Black South African Sample Using a Novel Software Program

Marisca Meyer *, Casper Hendrik Jonker, Sandeepa Rajbaran-Singh, Anna Catherina Oettlé

Posted Date: 7 May 2026

doi: 10.20944/preprints202605.0349.v1

Keywords: danger zone; safety zone; three-dimensional measurements; mesiobuccal root; distobuccal root; palatal root

 doi:10.20944/preprints202605.0349.v1

Article

Root Dentine Thickness of Maxillary First Molars in a Black South African Sample Using a Novel Software Program

Marisca Meyer [1,2,*], Casper Hendrik Jonker [3], Sandeepa Rajbaran-Singh [1] and Anna Catherina Oettle [2]

[1] Department of Maxillofacial and Oral Radiology, School of Dentistry, Sefako Makgatho Health Sciences University, Ga-Rankuwa, 0208, South Africa

[2] Anatomy and Histology Department, School of Medicine, Sefako Makgatho Health Sciences University, Ga-Rankuwa, 0208, South Africa

[3] Truro Dental Education Facility, Royal Cornwall Hospital, Knowledge Spa, Peninsula Dental School, Faculty of Health, University of Plymouth, Truro TR1 3HD, UK

* Correspondence: marisca.meyer@smu.ac.za

Abstract

Background/Objectives: Endodontic success in maxillary first molars is often complicated by their complex anatomy, increasing the risk of procedural errors in "danger zones" where dentine is thin. While global data on root morphology exists, population-specific information for South Africans is lacking. This study aims to quantify root dentine thickness in a Black South African sample using a novel software program to enhance accuracy for preoperative planning and improved clinical outcomes. **Methods:** Micro-CT scans of 97 maxillary first molars (57 individuals) were analyzed. Dentine thickness was measured at 0.1 mm intervals using a novel surface-to-interface software tool, which enabled automated, high-precision quantification of complex curved geometries. Data were standardized into 1 mm segments for analysis. Reliability trials confirmed high precision (within 0.0001 mm). **Results:** Buccal and lingual surfaces of mesiobuccal and distobuccal roots were consistently thicker than mesial and distal surfaces. All roots showed progressive thinning toward the apical third. Conversely, palatal roots exhibited an opposing pattern with mesial and distal surfaces that were thicker than buccal and lingual aspects. Age correlations were not statistically significant. **Conclusions:** The study identifies specific anatomical patterns in root dentine thickness within a South African sample. The thinner mesial and distal walls of buccal roots represent critical "danger zones" for clinicians. The novel software proved highly effective for precise morphometric mapping and offers a versatile framework for broader endodontic research. These findings provide essential data for optimizing endodontic treatment strategies and the development of population-specific dental instruments.

Keywords: danger zone; safety zone; three-dimensional measurements; mesiobuccal root; distobuccal root; palatal root

1. Introduction

Endodontic treatment as a dental restorative option refers to the dental management of a tooth demonstrating irreversible pulpitis (inflamed pulp), with the aim of retaining the tooth while eliminating infection and associated symptoms. In doing so, the tooth can continue to provide mechanical function and improve the quality of life of patients [1–3]. The procedure involves cleaning and shaping of root canals, chemical disinfection of the prepared root canal spaces and finally a three-dimensional seal of the prepared spaces to prevent re-infection [4]. Root canal treatment, when optimally completed, can save teeth that might otherwise need extraction [5].

 doi:10.20944/preprints202605.0349.v1

First molars are often susceptible to caries necessitating root canal treatments due to their early eruption and complex occlusal structure [6,7]. More specifically, the maxillary first molar has been extensively studied due to its three roots and complex and highly variable root canal anatomy, which presents significant challenges for successful endodontic treatment. The presence of a second mesiobuccal canal (MB2) on maxillary first molars is often difficult to detect and therefore commonly missed during treatment. Undetected canals may harbor microorganisms and necrotic tissue, potentially leading to persistent infection and endodontic failure thus rendering the maxillary first molar notoriously as one of the most difficult teeth to treat endodontically [8].

The success of these treatments depends on multiple factors and failure results in procedural complications such as perforations. Root perforations are defined as pathological communications between the root canal and surrounding periodontium which can arise during access preparation or cleaning and shaping, especially in areas with thin dentine known as “danger zones” [9–12]. Perforations may lead to inflammation, reinfection, periodontal damage, bone resorption or tooth loss and are estimated to account for up to 10% of root canal failures [13–15].

Root canals are typically irregular in shape (often flattened) causing irregular removal of tooth structure from root canal walls during the cleaning and shaping phase of endodontic treatment [16]. As root canal instruments have different tapers and designs, the amount of tooth structure removed will differ [17]. Subsequent post-space preparation further reduces root dentine thickness, which can increase the risk of perforation, ledging, or vertical root fractures if remaining dentine is insufficient [18,19]. Knowledge of relative spatial dentinal thickness is therefore crucial for minimizing procedural risks, particularly since the root canal, and most likely dentine, tapers from coronal to apical regions.

Traditionally, dentine thickness measurements have largely relied on manual assessment using two-dimensional imaging software that utilize cross-sections derived from three-dimensional datasets [18,20,21]. However, when evaluating complex, curved anatomical structures such as dental roots, these sections are often not consistently orthogonal to the local axis of the structure. This can introduce oblique measurement errors that misrepresent the actual surface-to-interface thickness. Consequently, there is a need for virtual sections that are adjustable according to the curvature of the surface. To overcome these challenges of inaccuracy and low repeatability, our study utilizes a novel software tool designed to automatically measure curved 3D structures. By generating adaptive virtual sections, that follow the natural curvature of the structure via a calculated centerline, this computational approach ensures consistent, automated thickness measurements across the entire model [22]. Adaptive virtual slices are produced by raycasting (from the Unity platform) to detect inner and outer surface boundaries. From each slice, radial lines are projected to compute perpendicular (true) thickness values at high resolution, after which the model is refined through smoothing and remeshing to correct artefacts. The system then produces both numerical outputs (e.g., mean, minimum, maximum thickness) and color-mapped visualizations of thickness distribution, enabling precise, reproducible analysis of complex anatomical forms [22].

Previous studies have often focused on specific roots or regions, such as only the mesiobuccal root of maxillary molars and typically examined only the first 4 mm below the furcation [7,23–26]. This study expands on previous work by measuring all sides/surfaces of all roots in maxillary first molars along the full root length. While dentinal thickness and canal morphology have been evaluated in various populations, there is limited data particularly in first molars derived from a South African population. To address these gaps in the literature, this study set out to determine the dentine thickness of the first maxillary molar roots in a Black South African sample using a novel software program.

Micro-computed tomography (micro-CT) imaging is used as it provides high-resolution three-dimensional imaging that allows precise assessment of dentine thickness without destructive sectioning. Because of its superior spatial resolution compared with conventional radiographic techniques, micro-CT studies often report more accurate and frequently smaller measurements of dentine thickness [27]. The findings of this study therefore aim to inform clinicians of accurate and

 doi:10.20944/preprints202605.0349.v1

repeatable population-specific variations in root dentine for preoperative planning, optimization of treatment strategies, and guide the design of endodontic instruments for improved outcomes.

2. Materials and Methods

In this cross-sectional, descriptive, quantitative study, micro-CT scans of 97 maxillary first molars from 57 individuals (26 males (between ages 24 and 62) and 31 females (between ages 22 and 70)) were analyzed. Where possible, left and right first molars from the same individual were included. The scans were retrospectively obtained from the dry skeletal collections of the Anatomy Departments of two universities in Gauteng Province, South Africa [28]. A convenience sampling strategy was employed.

Since a convenience sampling method was used, inclusion was based on scan availability. Scans were excluded if the first molars were poorly preserved, showed incomplete root formation, dentinal or enamel defects, root fractures, coronal or radicular resorption within the pulp–root complex, extensive caries that impeded accurate measurement, evidence of prior endodontic treatment, or metallic restorations (e.g., full or partial metal crowns, or porcelain-fused-to-metal crowns). Demographic data was available for all scans to allow for group comparisons.

The composition of the scan collection is presented in Table 1.

Table 1. Distribution of micro-CT samples of maxillary first molars.

	Left	Right	Total
Females	22	28	50
Males	25	22	47
Total	47	50	97

Measurement Software

The scans were uploaded into a novel surface-to-interface thickness measuring tool for curved biological structures [22] and analyzed accordingly. Once the thickness measurements of each scan were obtained, further data processing in Microsoft Excel was done. Thickness measurements for each root surface area (mesial, distal, buccal and lingual) were obtained in the program at 0.1 mm intervals along the length of each root. To standardize the data to 1 mm increments, every ten consecutive 0.1 mm measurements were grouped and averaged to yield a single representative thickness value per millimeter (Figure 1). Accordingly, measurements from 0.0–0.9 mm were averaged for the first millimeter segment, those from 1.0–1.9 mm for the second segment, and so forth along the root.

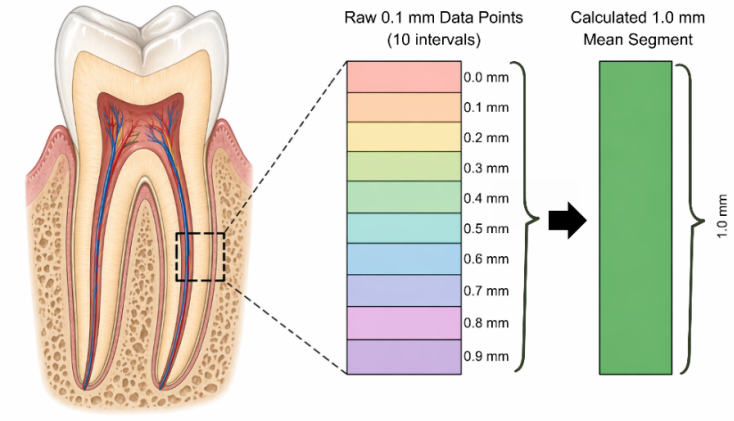

Figure 1. Process showing how 0.1 mm measurements were grouped and averaged to yield a single representative thickness value per mm.

 doi:10.20944/preprints202605.0349.v1

Statistical Analysis

To evaluate the reliability of the software tool, validation trials were conducted using ten computer-generated models. These models included cylindrical and cuboidal structures to represent the two geometric extremes commonly encountered in biological tissues. Since measurements were generated using computational methods, repeatability was confirmed without requiring multiple manual repetitions by the researcher.

Once the repeatability of the measurements had been established, statistical analyses were performed using PAST software version 4.11 [29]. Descriptive statistics were calculated for all root dentine thickness measurements obtained from the micro-CT scans to summarize central tendency and variability. The mean was used to indicate central tendency, while the standard deviation and range described data dispersion.

The Shapiro–Wilk test was applied to assess the normality of the data distribution, as this test is appropriate for small to moderate sample sizes typical of micro-CT–based anatomical studies. The assumption of normality was tested at a 5% significance level ($\alpha = 0.05$), under the null hypothesis that the data follows a normal distribution. If the null hypothesis was rejected, indicating non-normality, non-parametric statistical methods would have been applied for subsequent analyses.

For normally distributed data, paired t-tests were performed and for non-normally distributed data, the Wilcoxon signed-rank test was used to assess differences between left and right sides. Differences in root surface areas (mesial, distal, buccal, and lingual) as well as between levels (coronal, middle and apical third) were evaluated using repeated measures ANOVA for normally distributed data and the Friedman test for non-normally distributed data, with Bonferroni correction applied for multiple pairwise comparisons for non-normally distributed data. Differences between male and female groups were analyzed using independent samples t-test and the Mann–Whitney U test. To assess the relationship between root dentine thickness and age, Pearson's correlation coefficient was used for normally distributed variables, while Spearman's rank correlation coefficient was applied to non-normally distributed variables. A Bonferroni correction was applied where appropriate to adjust for multiple comparisons.

To further analyze the effect of ageing on dentine thickness, and to ensure that the influence of this variable was adequately accounted for, both post hoc and a priori power analyses were performed using the software G*Power [30]. A priori power analyses were performed to estimate the sample size required to have a high probability of detecting a statistically significant difference with ageing if it really had an influence on root dentine thickness of maxillary first molars using a set α of 0.05 and power of 0.80 consistent with conventions in biomedical research to balance sensitivity with feasibility [31]. Post hoc tests were performed to compute the achieved power of the correlation with aging at the sample size reached by convenience sampling and effect size at a set α of 0.05 as well as in the case of normal distribution, the Pearson's correlation coefficient (r) or the Spearman's rank-order correlation (rs) if non-parametric.

3. Results

3.1. Repeatability Results

The software produced consistent and highly accurate measurements across all models. For cylindrical shapes, accuracy was within 0.0001 mm, and for cuboidal shapes, the measurements were entirely precise.

3.2. Descriptive Statistics

Descriptive statistics are shown in Table 2 for the pooled data of the left distobuccal (DB), mesiobuccal (MB) and palatal root, respectively. The buccal and lingual surfaces consistently demonstrated greater thickness than the mesial and distal surfaces across all measured levels of the MB and DB roots, with a progressive reduction in dentine thickness from the coronal toward the

 doi:10.20944/preprints202605.0349.v1

apical third, where the apical third shows the greatest reduction in thickness. Standard deviations also increased apically, suggesting greater variability. Post-hoc analysis confirmed significant differences in wall thickness based on root orientation ($p < 0.05$). In the coronal and middle thirds (0 – 4 mm), the MB and DB roots exhibited a distinct pattern where the buccal and lingual surfaces were significantly thicker than the mesial and distal surfaces. While the mesial and distal walls of the palatal root remained statistically similar throughout, the MB and DB roots showed significant proximal asymmetry where mesial was statistically significantly different from distal in the first mm before becoming equal.

In contrast to the MB and DB roots, the palatal root exhibited an opposing distribution pattern. The mesial and distal surfaces of the palatal root were consistently thicker than the buccal and lingual aspects at most measured levels. Statistically, the palatal root exhibited significantly greater thickness along its mesial and distal walls throughout the coronal and middle thirds (0 – 6 mm). In these regions, the mesial and distal walls outweighed the buccal and lingual surfaces ($p < 0.05$), though they remained statistically comparable to one another. Similar to the MB root, this gap gradually resolved toward the apical region, eventually reaching statistical uniformity across all surfaces at the 8 mm level ($p > 0.05$).

Furthermore, although a progressive reduction in dentine thickness toward the apical third was evident, the palatal root maintained comparatively greater overall thickness than the MB and DB roots.

Table 2. Dentine thickness of pooled data of all three left maxillary roots.

Root		Distobuccal (DB)					Mesiobuccal (MB)					Palatal				
	Area	M	D	L	B	Significant differences	M	D	L	B	Significant differences	M	D	L	B	Significant differences
Dentine thickness (mm)	0	N=44 **1.25** *0.16*	N=44 **1.42** *0.15*	N=44 **1.84** *0.20*	N=44 **1.83** *0.17*	M ≠ D ≠ (L ≈ B)	N=44 **1.47** *0.17*	N=44 **1.28** *0.18*	N=44 **2.08** *0.22*	N=44 **2.16** *0.22*	M ≠ D ≠ (L ≈ B)	N=46 **2.09** *0.25*	N=46 **2.15** *0.24*	N=46 **1.72** *0.19*	N=46 **1.66** *0.23*	(M ≈ D) ≠ (L ≈ B)
	1	N=44 **1.22** *0.17*	N=44 **1.36** *0.15*	N=44 **1.75** *0.22*	N=44 **1.71** *0.17*	M ≠ D ≠ (L ≈ B)	N=44 **1.38** *0.17*	N=44 **1.25** *0.18*	N=44 **2.00** *0.24*	N=44 **2.03** *0.24*	M ≠ D ≠ (L ≈ B)	N=46 **2.00** *0.25*	N=46 **2.06** *0.25*	N=46 **1.63** *0.18*	N=46 **1.61** *0.23*	(M ≈ D) ≠ (L ≈ B)
	2	N=44 **1.19** *0.18*	N=44 **1.28** *0.17*	N=44 **1.64** *0.24*	N=44 **1.58** *0.19*	(M ≈ D) ≠ (L ≈ B)	N=44 **1.32** *0.17*	N=44 **1.22** *0.21*	N=44 **1.91** *0.28*	N=44 **1.92** *0.26*	(M ≈ D) ≠ (L ≈ B)	N=46 **1.90** *0.26*	N=46 **1.96** *0.27*	N=46 **1.55** *0.16*	N=46 **1.56** *0.24*	(M ≈ D) ≠ (L ≈ B)
	3	N=44 **1.13** *0.20*	N=44 **1.19** *0.21*	N=44 **1.49** *0.28*	N=44 **1.43** *0.23*	(M ≈ D) ≠ (L ≈ B)	N=44 **1.26** *0.18*	N=44 **1.22** *0.21*	N=44 **1.79** *0.30*	N=44 **1.81** *0.27*	(M ≈ D) ≠ (L ≈ B)	N=46 **1.78** *0.27*	N=46 **1.83** *0.30*	N=46 **1.48** *0.17*	N=46 **1.47** *0.27*	(M ≈ D) ≠ (L ≈ B)
	4	N=44 **1.00** *0.25*	N=44 **1.05** *0.28*	N=44 **1.28** *0.34*	N=44 **1.22** *0.31*	(M ≈ D) ≠ (L ≈ B)	N=44 **1.21** *0.20*	N=44 **1.16** *0.23*	N=44 **1.62** *0.35*	N=44 **1.67** *0.28*	(M ≈ D) ≠ (L ≈ B)	N=46 **1.61** *0.29*	N=46 **1.66** *0.37*	N=46 **1.35** *0.23*	N=46 **1.34** *0.31*	(M ≈ D) ≠ (L ≈ B)
	5	N=41 **0.88** *0.30*	N=41 **0.91** *0.35*	N=41 **1.06** *0.39*	N=41 **1.02** *0.36*	M ≈ D ≈ L ≈ B	N=44 **1.11** *0.24*	N=44 **1.00** *0.30*	N=44 **1.33** *0.44*	N=44 **1.50** *0.34*	(M ≈ D) ≠ L ≠ B	N=45 **1.37** *0.36*	N=45 **1.44** *0.44*	N=45 **1.17** *0.36*	N=45 **1.19** *0.31*	(M ≈ D) ≠ (L ≈ B)
	6	N=30 **0.75** *0.35*	N=30 **0.85** *0.37*	N=30 **0.90** *0.39*	N=30 **0.89** *0.39*	M ≈ D ≈ L ≈ B	N=41 **1.00** *0.25*	N=41 **0.87** *0.35*	N=41 **1.06** *0.49*	N=41 **1.28** *0.35*	M ≈ D ≈ L ≠ B	N=37 **1.18** *0.35*	N=37 **1.26** *0.41*	N=37 **1.12** *0.34*	N=37 **0.94** *0.31*	(M ≈ D) ≠ B; L ≈ all
	7	N=18 **0.75** *0.33*	N=18 **0.83** *0.36*	N=18 **0.83** *0.41*	N=18 **0.90** *0.42*	M ≈ D ≈ L ≈ B	N=35 **0.88** *0.29*	N=35 **0.73** *0.36*	N=35 **0.89** *0.45*	N=35 **1.01** *0.40*	M ≈ D ≈ L ≠ B	N=33 **1.00** *0.32*	N=33 **0.95** *0.42*	N=33 **1.00** *0.40*	N=33 **0.72** *0.31*	(M ≈ L) ≠ B; D ≈ all
	8	N=11 **0.63** *0.37*	N=11 **0.86** *0.35*	N=11 **0.76** *0.44*	N=11 **0.84** *0.37*	M ≈ D ≈ L ≈ B	N=22 **0.79** *0.28*	N=22 **0.67** *0.34*	N=22 **0.80** *0.42*	N=22 **0.94** *0.41*	M ≈ D ≈ L ≈ B	N=17 **0.88** *0.28*	N=17 **0.73** *0.35*	N=17 **0.85** *0.40*	N=17 **0.63** *0.31*	M ≈ D ≈ L ≈ B
	9	N=6 **0.60** *0.40*	N=6 **0.80** *0.46*	N=6 **0.75** *0.49*	N=6 **0.77** *0.42*	M ≈ D ≈ L ≈ B	N=12 **0.71** *0.30*	N=12 **0.63** *0.33*	N=12 **0.72** *0.36*	N=12 **0.86** *0.36*	M ≈ D ≈ L ≈ B	N=6 **0.75** *0.46*	N=6 **0.61** *0.28*	N=6 **1.01** *0.52*	N=6 **0.42** *0.28*	M ≈ D ≈ L ≈ B
	10	N=3 **0.60** *0.49*	N=3 **0.81** *0.53*	N=3 **0.71** *0.48*	N=3 **0.74** *0.48*	M ≈ D ≈ L ≈ B	N=7 **0.58** *0.35*	N=7 **0.57** *0.26*	N=7 **0.55** *0.41*	N=7 **0.83** *0.30*	M ≈ D ≈ L ≈ B	N=2 **1.31** *0.09*	N=2 **0.28** *0.01*	N=2 **1.11** *0.62*	N=2 **0.47** *0.27*	Insufficient data
	11	N=1 **0.66** *0.00*	N=1 **1.07** *0.00*	N=1 **0.44** *0.00*	N=1 **0.97** *0.00*	Insufficient data	N=2 **0.83** *0.39*	N=2 **0.39** *0.26*	N=2 **0.57** *0.06*	N=2 **0.72** *0.74*	Insufficient data					

 doi:10.20944/preprints202605.0349.v1

12	N=1 **0.54** *0.00*	N=1 **0.57** *0.00*	N=1 **0.89** *0.00*	N=1 **0.24** *0.00*	Insufficient data	N=1 **0.89** *0.00*	N=1 **0.37** *0.00*	N=1 **0.40** *0.00*	N=1 **0.94** *0.00*	Insufficient data
13						N=1 **0.67** *0.00*	N=1 **0.07** *0.00*	N=1 **0.34** *0.00*	N=1 **0.42** *0.00*	Insufficient data

N = number of roots. **Bold** = mean thickness. *Italics* = standard deviation. M = Mesial; D = Distal; L = Lingual; B = Buccal. ≈ statistically insignificant, ≠ statistically significant.

Neither the paired t-tests nor the Wilcoxon signed-rank test showed statistically significant differences between left and right sides; thus all further testing was only performed on one side (left). No statistically significant differences were observed between males and females while using the independent samples t-test and Mann Whitney U test. Consequently, the data were pooled, and analyses on the different root surface areas and levels, as well as age correlation analyses were conducted on the combined sample.

Repeated measures ANOVA and the Friedman test were performed on the pooled groups and demonstrated statistically significant differences in root surface areas (mesial, distal, buccal, and lingual) for most slices of each root (Table 2; Figure 2) as well as between levels (coronal, middle and apical third).

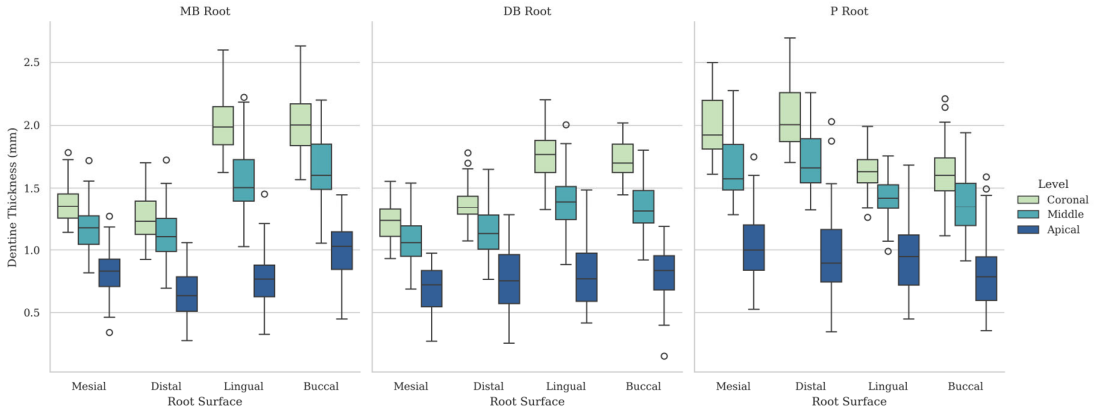

Figure 2. Comparison of dentine thickness (mm) across four root surfaces (mesial, distal, buccal, and lingual) at the coronal, middle, and apical thirds for the MB, DB, and P roots of maxillary first molars.

Where a significant overall difference was identified, post hoc pairwise comparisons were conducted to determine which surfaces differed. The analyses revealed a significant and progressive reduction in dentine thickness across all four surfaces of the maxillary molar roots as they transitioned from the coronal to the apical third. Statistically, for all three roots, the wall thickness at the coronal third was significantly greater than at the middle third, which was in turn significantly thicker than the apical third ($p < 0.05$). Furthermore, a comparison between the coronal and apical thirds revealed an extremely significant reduction in overall dentine thickness across all root types ($p < 0.001$), confirming the substantial narrowing of the root structure toward the apex (Figure 3).

 doi:10.20944/preprints202605.0349.v1

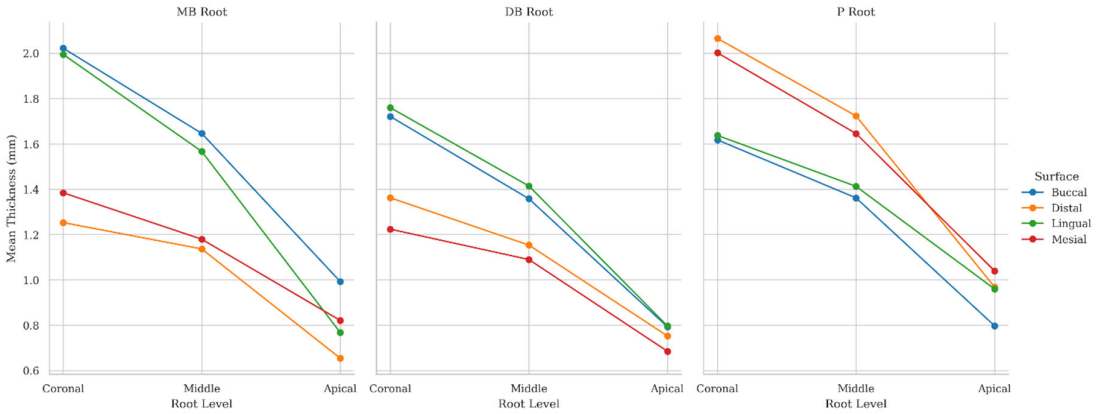

Figure 3. Linear profile plot demonstrating the mean dentine thickness reduction from the coronal to the apical third. Each line represents a specific root surface.

This consistent pattern of thinning indicates a predictable longitudinal tapering of the root walls regardless of the specific root or surface measured. In the MB and DB roots, the buccal and lingual walls represented the thickest structural components in the coronal and middle regions. While these surfaces remained the thickest throughout the root's length, the gap between these and the thinner mesial and distal walls reduced as the root progressed apically.

However, the palatal root displayed a different morphological distribution in its upper regions. In the coronal and middle thirds, the mesial and distal walls were significantly thicker than the buccal and lingual walls. Though, much like the buccal roots, this internal gap resolved in the apical region. By the 8 mm level (apical third), all three roots did not differ statistically across all four surfaces.

Neither Pearson's nor Spearman's correlation analyses demonstrated statistically significant associations between root dentine thickness and age. While the majority of correlation coefficients indicated weak positive relationships, several weak negative correlations were also present and often observed in the apical third of the dental root indicated as T3 in Table 3. The power analyses revealed that in some instances, adequate sample sizes were achieved to demonstrate correlations with ageing, e.g. in the coronal third of the lingual side of roots. In a few correlations very high sample numbers (in the thousands) were needed to have a high probability of detecting a statistically significant difference with ageing if it really had an influence on root dentine thickness of maxillary first molars. In three correlations situated in the coronal third of roots, effect size of ageing reached a moderately positive strength with strong statistical power (> 0.8), while the remainder of the correlations were weak, not statistically significant and had a low power.

Table 3. Power analysis of the effect of aging on the root dentine thickness of maxillary first molars.

SIDE/LEVEL → ROOT ↓	**Mesial T1**	**Mesial T2**	**Mesial T3**	**Distal T1**	**Distal T2**	**Distal T3**	**Lingual T1**	**Lingual T2**	**Lingual T3**	**Buccal T1**	**Buccal T2**	**Buccal T3**
DB N = 44	**0.2229**	**0.1267**	***0.1354***	**0.2300**	**0.2685**	**-0.0062**	**0.2703**	**0.2420**	**0.1341**	**0.1380**	**0.0752**	**-0.2601**
	155	486	*425*	146	106	203887	16	104	342	323	1093	90
	0.4301	0.2055	*0.2222*	0.3973	0.5557	0.0542	0.5608	0.4822	0.2197	0.2273	0.1231	0.5323
MB N = 44	***0.0111***	**0.1544**	**0.0950**	**0.3856**	**0.2754**	**0.0987**	**0.3188**	**0.2614**	**0.1069**	**0.2187**	**0.2249**	**0.0523**
	63989	327	866	50	101	803	29	22	539	127	120	2261
	0.0578	0.2614	0.1515	0.8400	0.5748	0.1572	0.6910	0.5361	0.1705	0.4189	0.4354	0.0954
P N = 46	***0.2859***	***0.2630***	**-0.0734**	***0.2630***	**0.2783**	***0.1746***	**0.1881**	**0.1837**	***-0.1089***	**0.1331**	**0.1473**	***0.1809***
	93	*111*	1455	*111*	99	*255*	30	181	*520*	347	283	*187*
	0.6211	*0.2692*	0.1230	*0.5567*	0.5998	*0.3167*	0.3506	0.3394	*0.1780*	0.2238	0.2536	*0.3325*
Mesial N = 37	**-0.1012**	***-0.0173***	**0.2563**	**0.4589**	**0.0918**	**-0.1671**	**0.0877**	**-0.0697**	**-0.1746**	**0.1612**	**0.0231**	***-0.0553***
	764	*26129*	117	34	929	38	802	1272	201	236	11623	*2019*
	0.2408	*0.0613*	0.4626	0.9021	0.1348	0.2577	0.1296	0.1084	0.2730	0.2464	0.0655	*0.0934*
Distal	**0.3981**	**0.2739**	***0.1671***	**0.2220**	***0.1238***	**0.0139**	**0.2738**	**0.0856**	**-0.0354**	**0.1589**	**0.1220**	**-0.1738**

 doi:10.20944/preprints202605.0349.v1

N = 37	47	102	*278*	157	*509*	5141	81	842	4929	243	414	203
	0.9993	0.5074	*0.2580*	0.3779	*0.1808*	0.0589	0.5072	0.1270	0.0753	0.2420	0.1779	0.2713

N = number of roots. T1: coronal third; T2: middle third; T3: apical third. First bold value in each cell: coefficient of correlation: r or rs (effect size). Second underlined value in each cell: A priori: required sample size. Third value in each cell: Post hoc: Power analysis. Cursive entries indicate non normal distributions based on Spearman rs.

4. Discussion

The present study established a baseline for root dentine thickness in a Black South African sample - a demographic that has been underrepresented in endodontic morphological research. In contrast to earlier studies that concentrated on selected roots or assessed only the initial few millimeters apical to the furcation, the present study offers a comprehensive mapping of the mesiobuccal (MB), distobuccal (DB), and palatal roots at 1-mm intervals along their full lengths. By using micro-CT technology and a novel software program, we were able to document the intricate tapering of dentine from the coronal to the apical areas with high accuracy.

A critical finding of this study relates to the identification of "danger zones," where dentine is naturally thinner and more susceptible to procedural complications. The results indicated that the distal aspect of the MB root and the mesial aspect of the DB root consistently displayed lower mean thickness values, especially towards the apical portion of the root. These areas represent significant risks for strip perforations during mechanical cleaning and shaping. These findings align with the "danger zone" concept originally introduced by Abou-Rass (1980) [32] and recent morphometric analyses that identify the distal wall of mesial roots as having the thinnest dentine, often measuring less than 1.0 mm [7,33]. Specifically, while some studies locate the minimum thickness 1–2 mm below the furcation [7], our results suggest that this vulnerability is also pronounced in the apical third, where radicular dentine thickness is significantly lower compared to the coronal regions [34]. Furthermore, since post-space preparation inevitably decreases the amount of remaining dentine, these findings highlight the need for careful clinical judgement to minimize the risk of vertical root fractures or unintended communication with the periodontium.

A notable finding of this study is the contrasting distribution pattern observed in the palatal root compared to the buccal roots. While the MB and DB roots exhibited critical thinning on their mesial and distal surfaces, the palatal root maintained significantly greater thickness along these same walls throughout the coronal and middle thirds. This distinct anatomical configuration likely reflects the palatal root's broader mesiodistal dimension and aligns with established anatomical descriptions of its robust canal morphology [8,35]. For the clinician, this implies that while the proximal walls of buccal roots represent high-risk 'danger zones,' the palatal root offers a greater margin of safety during proximal instrumentation.

Our longitudinal mapping further revealed a significant merging of wall thickness as the roots progressed apically. Although regional asymmetries were pronounced in the coronal regions, these gaps gradually resolved, with all three roots reaching statistical uniformity across all four surfaces at the 8 mm level. This suggests that the specialized 'danger zones' identified in the upper two-thirds of the root essentially merge into a universal high-risk zone at the apex. Consequently, regardless of the initial coronal dimensions or root type, the entire apical circumference must be treated with equal caution to prevent unintended communication with the periodontium [36].

Statistical analysis using paired t-tests and the Wilcoxon signed-rank test revealed no significant differences in dentine thickness between the left and right maxillary first molars. This suggests a high degree of bilateral symmetry, allowing clinicians to potentially use the morphology of a contralateral tooth as a reliable guide for preoperative planning. Additionally, no statistically significant differences were observed between male and female groups. Interestingly, correlation analyses also did not demonstrate statistically significant associations between age and dentine thickness.

Another important factor to consider is ageing, particularly in the growing elderly population requiring restorative dental care. Age-related deposition of secondary dentine along the root canal

 doi:10.20944/preprints202605.0349.v1

walls is a well-established phenomenon, resulting in progressive narrowing and potential obliteration of the canal space. This process is continuous throughout life and strongly correlated with chronological age, leading to morphological alterations such as reduced canal diameter and increased dentine thickness in older individuals [37–40]. Although the majority of regions in the current study demonstrated weak positive correlations between age and dentine thickness, isolated negative correlations were observed within specific apical regions (Table 3) which suggests that apical anatomy remains high-risk regardless of patient age. Despite the fact that the age distribution and small size of samples could have influenced the findings on age correlations, it may also suggest complex, population-specific patterns of dentine deposition or resorption that differ from the generalized expectation of continuous secondary dentine formation with age [41–44]. This underscores the necessity for rigorous preoperative planning for all patients, as increased age does not necessarily guarantee a 'safer' or thicker apical dentine wall.

Several potential explanations may account for the absence of a clear or consistent pattern in the influence of ageing on dentine thickness across the root. These thickness variations likely reflect a combination of adaptive and age-related changes within the root structure. Rather than a uniform process, secondary dentine deposition appears to be influenced by localized biomechanical loading, where root surfaces undergo asymmetric reinforcement in response to occlusal stress [45,46]. This remodeling is further complicated by physiological aging, as variable cementum deposition and minor apical resorption can subtly alter measurable dentine thickness over time [41,43]. Consequently, the final root morphology is not a fixed shape, but rather the result of a lifetime of functional demands and structural wear [42,44]. In addition, the apical third is anatomically more variable and typically exhibits thinner dentinal walls compared to coronal regions [35,36], making measurements in this region more susceptible to slight segmentation inconsistencies or methodological sensitivity when assessed using imaging modalities [47,48]. Sampling variation and small effect sizes may also contribute to weak negative correlations. Given that these correlations were of low magnitude, statistically not significant and largely limited to anatomically variable apical regions, they are unlikely to represent a biologically meaningful age-related reduction in dentine thickness.

When comparing the results of this South African sample to international literature, notable variations emerge. For instance, at 2 mm and 3 mm from the furcation, our pooled MB root measurements (approximately 1.22 mm to 1.32 mm for the mesial/distal walls) align closely with some findings from Brazilian samples yet differ from the smaller values reported in certain Iranian and Turkish studies (Table 4). These variations underscore the importance of population-specific data.

Table 4. Studies conducted on dentine thickness of maxillary first molars.

Author, year of study and location	Root/s	Measurement modalities	Location of sections	Measurements in mm
Ordinola-Zapata et al., 2019 [24] Brazil	100 extracted mesiobuccal roots of maxillary first molars	Micro-CT	Median distances at: 2 mm 3 mm from furcation towards apex	Distance to distal wall MB1: 1.26; MB2: 1.00 MB1: 1.24; MB2: 0.99
			2 mm 3 mm from furcation towards apex	Distance to mesial wall MB1: 1.40; MB2: 1.20 MB1: 1.33; MB2: 1.17
Azimi et al., 2020 [49] Iran	50 intact mesiobuccal roots of maxillary first molars	CBCT	0 mm 2 mm 4 mm from furcation towards apex	Distance to distal wall MB1: 1.01; MB2: 0.90 MB1: 1.02; MB2: 0.91 MB1: 0.90; MB2: 0.81
Yanık and Nalbantoğlu, 2022 [50] Türkiye	642 intact mesiobuccal roots of maxillary first molars	CBCT	Median distances at 3 mm from furcation towards apex	Distance to distal wall: MB1: 0.83 mm; MB2: 0.80 mm Distance to mesial wall: MB1: 0.97 mm; MB2: 0.91 mm

 doi:10.20944/preprints202605.0349.v1

The differences in observed values across these studies may be attributed to both population-specific anatomy and the methodologies employed. Previous investigations [49,50] primarily utilized clinical CBCT with voxel sizes between 0.1 mm and 0.2 mm, relying on manual 2D linear measurements at predetermined levels. In contrast, the current study utilized high-resolution micro-CT paired with an automated 3D thickness mapping tool [22]. While manual 2D measurements are limited to specific cross-sectional slices, the automated raycasting approach evaluates the entire curved surface. This allows for the identification of the absolute thinnest point of the 'danger zone' which may be overlooked by traditional sampling at fixed intervals.

The use of our novel software program proved to be a significant methodological strength, yielding highly accurate and repeatable measurements. Validation trials on computer-generated models showed precision within 0.0001 mm for cylindrical shapes and perfect precision for cuboidal shapes. This level of accuracy, combined with the non-destructive nature of micro-CT scanning, allowed for a more robust analysis than traditional 2D radiography or manual sectioning. By standardizing measurements at 0.1 mm intervals and averaging them into 1 mm segments, the study provides a granular yet clinically applicable dataset.

The high resolution of the novel software tool allowed for the detection of subtle morphological changes that traditional 2D methods might overlook. Specifically, the identification of significant proximal asymmetry within the first millimeter of the MB and DB roots (where mesial and distal thicknesses differed momentarily before becoming equal) highlights the value of standardizing measurements at 0.1 mm intervals. This level of granularity ensures that even localized thinning at the very onset of the root canal is captured, providing a more precise baseline for the development of population-specific dental instruments [24,47].

Despite the insights gained, this study was limited by its reliance on a convenience sampling strategy from dry skeletal collections. The relatively small sample size could have obscured some findings e.g. the effect of aging on dentine thicknesses. Furthermore, while demographic data were available, the retrospective nature of the scans means that certain systemic or environmental factors affecting the living subjects could not be fully controlled. The study's scope was also restricted by its focus on a single South African population group and the use of dry skeletal remains. Furthermore, while the isotropic voxel resolution (62.4 μm to 74.2 μm) might be viewed as a constraint, it aligns with the 75 μm – 80 μm range recommended by Bai et al. (2023) [51] for optimal diagnostic accuracy.

A significant strength of this methodology was the use of software-driven segmentation; this approach improved data precision and facilitated a detailed comparative analysis of root canal morphology across sex, age, and dental arches. Future research should aim to expand this database to include other tooth types within the South African population. Applying this novel software to a broader range of dental morphologies will further enhance the development of population-specific endodontic instruments and treatment strategies.

5. Conclusions

This study successfully established a 3D baseline for root dentine thickness of first molars in a Black South African sample, bridging a gap in current dental morphological literature. By mapping all three roots of the maxillary first molar across their length, this research confirmed the critical "danger zones" on the distal aspect of the MB root and the mesial aspect of the DB root, where dentine is the thinnest and the risk of perforation is the highest while relatively sparing the palatal root.

The lack of significant sexual dimorphism and high degree of bilateral symmetry suggest that these anatomical findings can be applied generally within this population to improve preoperative planning. Negative age-related correlations in the apical third also question traditional assumptions about secondary dentine deposition, emphasizing that apical anatomy remains high-risk regardless of patient age. In summary, the results provide clinically relevant insight that could facilitate safer instrumentation and promote improved long-term retention of treated teeth. Furthermore, these findings can be integrated into dental school curricula to improve how students are taught to navigate complex canal systems. By using 3D models to identify thin areas of dentine, both undergraduate

 doi:10.20944/preprints202605.0349.v1

and postgraduate students can better prepare for the mechanical challenges of cleaning and shaping, leading to fewer clinical complications.

Author Contributions: Conceptualization, C.H.J.; methodology, M.M., A.C.O. and C.H.J.; validation, M.M., A.C.O. and C.H.J.; formal analysis, M.M. and A.C.O.; investigation, M.M.; resources, C.H.J., A.C.O., S.R.-S. and M.M.; data curation, M.M., A.C.O. and C.H.J.; writing—original draft preparation, M.M.; writing—review and editing, S.R.-S., A.C.O., and C.H.J.; visualization, S.R.-S., A.C.O., C.H.J., and M.M.; supervision, S.R.-S., A.C.O. and C.H.J.; project administration, A.C.O.; funding acquisition, S.R.-S. All authors have read and agreed to the published version of the manuscript.

Funding: This study was supported by the National Research Foundation (NRF) under the Research Development Grants for New Generation of Academics Program (nGAP) [Grant No: NGAP240205203589] and co-funded by the Department of Higher Education and Training (DHET) through the Staffing South African Universities Framework (SSAUF) and nGAP.

Institutional Review Board Statement: Ethical approval for this study was obtained from the School of Medicine Research Committee of the Sefako Makgatho Health Sciences Univer sity (SREC) and the Sefako Makgatho Health Sciences University Ethics Committee (SMUREC) (SMUREC/M/443/2024:PG) (13 February 2025), ensuring adherence to the guidelines for research involving human subjects. Informed Consent Statement: Informed consent from patients was not possible as Micro-CT scans from skulls of deceased individuals were used. Permission for research was given by family members in the case of a donation, and unclaimed bodies are protected by the National Health Act 61 of 2012.

Data Availability Statement: The data presented in this study are available from the corresponding author upon request. The data is not publicly available due to ethical reasons.

Conflicts of Interest: The authors declare no conflicts of interest.

References

1. Iqbal, M.K.; Kim, S. For teeth requiring endodontic treatment, what are the differences in outcomes of restored endodontically treated teeth compared to implant-supported restorations? *Int. J. Oral Maxillofac. Implants* **2007**, *22*, 96–113.
2. Chourasia, H.R.; Meshram, G.K.; Warhadpande, M.; Dakshindas, D. Root canal morphology of mandibular first permanent molars in an Indian population. *Int. J. Dent.* **2012**, *2012*, 745152.
3. Buchanan, G.D.; Gamieldien, M.Y.; Tredoux, S.; Vally, Z.I. Root and canal configurations of maxillary premolars in a South African subpopulation using cone beam computed tomography and two classification systems. *J. Oral Sci.* **2020**, *62*, 93–97.
4. Vertucci, F.J. Root canal morphology and its relationship to endodontic procedures. *Endod. Top.* **2005**, *10*, 3–29.
5. De Moor, R.J.G.; Deroose, C.A.; Calberson, F.L.G. The radix entomolaris in mandibular first molars: an endodontic challenge. *Int. Endod. J.* **2004**, *37*, 789–799.
6. Bjørndal, L.; Laustsen, M.H.; Reit, C. Root canal treatment in Denmark is most often carried out in carious vital molar teeth and retreatments are rare. *Int. Endod. J.* **2006**, *39*, 785–790.
7. Zhou, G.; Leng, D.; Li, M.; Zhou, Y.; Zhang, C.; Sun, C.; Wu, D. Root dentine thickness of danger zone in mesial roots of mandibular first molars. *BMC Oral Health* **2020**, *20*, 43.
8. Jonker, C.H.; van der Vyver, P.J.; Oettlé, A.C. Root and canal morphology of the maxillary first molar: A micro-computed tomography-focused review of literature with illustrative cases: Part 1: External root morphology. *S. Afr. Dent. J.* **2024**, *79*, 7–10.
9. Davis, G.R.; Tayeb, R.A.; Seymour, K.G.; Cherukara, G.P. Quantification of residual dentine thickness following crown preparation. *J. Dent.* **2012**, *40*, 571–576.
10. Lee, K.W.; Kim, Y.; Perinpanayagam, H.; Lee, J.K.; Yoo, Y.J.; Lim, S.M.; Chang, S.W.; Ha, B.H.; Zhu, Q.; Kum, K.Y. Comparison of alternative image reformatting techniques in micro-computed tomography and tooth clearing for detailed canal morphology. *J. Endod.* **2014**, *40*, 417–422.

 doi:10.20944/preprints202605.0349.v1

11. Tabassum, S.; Khan, F.R. Failure of endodontic treatment: the usual suspects. *Eur. J. Dent.* **2019**, *13*, 144–147.
12. Sarao, S.K.; Berlin-Broner, Y.; Levin, L. Occurrence and risk factors of dental root perforations: a systematic review. *Int. Dent. J.* **2020**, *71*, 96–105.
13. Ng, Y.L.; Mann, V.; Gulabivala, K. A prospective study of the factors affecting outcomes of nonsurgical root canal treatment: part 1: periapical health. *Int. Endod. J.* **2011**, *44*, 583–609.
14. Saed, S.M.; Ashley, M.P.; Darcey, J. Root perforations: aetiology, management strategies and outcomes. The hole truth. *Br. Dent. J.* **2016**, *220*, 171–180.
15. Clauder, T. Present status and future directions – Managing perforations. *Int. Endod. J.* **2022**, *55*, 872–891.
16. Versiani, M.A.; Pécora, J.D.; Sousa-Neto, M.D. A micro-computed tomography study of the root canal morphology of single-rooted maxillary canines. *Int. Endod. J.* **2011**, *44*, 1062–1072.
17. Versiani, M.A.; Ordinola-Zapata, R.; Keleş, A.; Alcin, H.; Bramante, C.M.; Pécora, J.D.; Sousa-Neto, M.D. Middle mesial canals in mandibular first molars: a micro-CT study in different populations. *Arch. Oral Biol.* **2016**, *61*, 130–137.
18. Lim, S.S.; Stock, C.J.R. The risk of perforation in the curved canal: anticurvature filing compared with the stepback technique. *Int. Endod. J.* **1987**, *20*, 33–39.
19. Subramanian, P.; Al-Marzok, M.I.K.; Murugeshappa, D.G.; Kacharaju, K.R.; Mohamad Hanapi, N.S.; Nambiar, P. Comparative evaluation of the remaining dentin thickness using different root canal retreatment techniques: a cone-beam computed tomography study. *J. Int. Dent. Med. Res.* **2021**, *14*, 901–909.
20. Berutti, E.; Fedon, G. Thickness of cementum/dentin in mesial roots of mandibular first molars. *J. Endod.* **1992**, *18*, 545–548.
21. Bissinger, O.; Probst, F.A.; Wolff, K.D.; Jeschke, A.; Weitz, J.; Deppe, H.; Kolk, A. Comparative 3D micro-CT and 2D histomorphometry analysis of dental implant osseointegration in the maxilla of minipigs. *J. Clin. Periodontol.* **2017**, *44*, 418–427.
22. Meyer, M.; Potgieter, R.; Jonker, C.H.; Rajbaran-Singh, S.; Oettlé, A.C. Outer shell thickness measuring tool for structures with curved surfaces. *Research Square* **2026**, preprint (in press).
23. Sauaia, T.S.; Gomes, B.P.F.A.; Pinheiro, E.T.; Zaia, A.A.; Ferraz, C.C.R.; Souza-Filho, F.J.; Valdrighi, L. Thickness of dentine in mesial roots of mandibular molars with different lengths. *Int. Endod. J.* **2010**, *43*, 555–559.
24. Ordinola-Zapata, R.; Martins, J.N.R.; Versiani, M.A.; Bramante, C.M. Micro-CT analysis of danger zone thickness in the mesiobuccal roots of maxillary first molars. *Int. Endod. J.* **2019**, *52*, 524–529.
25. De-Deus, G.; Rodrigues, E.A.; Belladonna, F.G.; Simões-Carvalho, M.; Cavalcante, D.M.; Oliveira, D.S.; Souza, E.M.; Giorgi, K.A.; Versiani, M.A.; Lopes, R.T.; Silva, E.J.N.L.; Paciornik, S. Anatomical danger zone reconsidered: a micro-CT study on dentine thickness in mandibular molars. *Int. Endod. J.* **2019**, *52*, 1501–1507.
26. Keleş, A.; Keskin, C.; Alqawasmi, R.; Versiani, M.A. Evaluation of dentine thickness of middle mesial canals of mandibular molars prepared with rotary instruments: a micro-CT study. *Int. Endod. J.* **2020**, *53*, 519–528.
27. Meyer, M.; Oettle, A.C.; Jonker, C.H.; Rajbaran-Singh, S. Dentine thicknesses of first molar roots: A review of the literature with illustrative cases. *S. Afr. Dent. J.* **2025**, *80*, 95–103.
28. L'Abbé, E.N.; Krüger, G.C.; Theye, C.E.; Hagg, A.C.; Sapo, O. The Pretoria Bone Collection: A 21st Century Skeletal Collection in South Africa. *J. Forensic Sci.* **2021**, *1*, 220–227.
29. Hammer, Ø.; Harper, D.A.T.; Ryan, P.D. PAST: Paleontological statistics software package for education and data analysis. *Palaeontol. Electron.* **2001**, *4*, 1–9.
30. Faul, F.; Erdfelder, E.; Lang, A.G.; Buchner, A. G* Power 3: A flexible statistical power analysis program for the social, behavioral, and biomedical sciences. *Behav. Res. Methods* **2007**, *39*, 175–191.
31. Biau, D.J.; Kernéis, S.; Porcher, R. Statistics in brief: the importance of sample size in the planning and interpretation of medical research. *Clin. Orthop. Relat. Res.* **2008**, *466*, 2282–2288.
32. Abou-Rass, M.; Frank, A.L.; Glick, D.H. The anticurvature filing method to prepare the curved root canal. *J. Am. Dent. Assoc.* **1980**, *101*, 792–794.

 doi:10.20944/preprints202605.0349.v1

33. Bolbolian, M.; Ramezani, M.; Valadabadi, M.; Alizadeh, A.; Tofangchiha, M.; Ghonche, M.R.A.; Reda, R.; Zanza, A.; Testarelli, L. Dentin Thickness of the Danger Zone in the Mesial Roots of the Mandibular Molars: A Cone Beam Computed Tomography Analysis. *Front. Biosci.-Schol.* **2023**, *15*, 1.
34. Arılı-Öztürk, E.; Büyükgöze-Dindar, M. Evaluation of Radicular Dentin Thickness in Maxillary and Mandibular Central Incisor, Canine, and Premolar Teeth. *Cureus* **2024**, *16*, e56974.
35. Vertucci, F.J. Root canal anatomy of the human permanent teeth. *Oral Surg. Oral Med. Oral Pathol.* **1984**, *58*, 589–599.
36. Wu, M.K.; Wesselink, P.R.; Walton, R.E. Apical terminus location of root canals. *Int. Endod. J.* **2000**, *33*, 395–399.
37. Hisham, S.; Abdullah, N.; Noor, M.H.M.; Franklin, D. Quantification of secondary dentin formation based on the analysis of MDCT scans and dental OPGs in a contemporary Malaysian population. *Legal Med.* **2019**, *36*, 59–66.
38. Maeda, H. Aging and senescence of dental pulp and hard tissues of the tooth. *Front. Cell Dev. Biol.* **2020**, *8*, 605996.
39. Solomonov, M.; Kim, H.C.; Hadad, A.; Levy, D.H.; Itzhak, J.B.; Levinson, O.; Azizi, H. Age-dependent root canal instrumentation techniques: a comprehensive narrative review. *Restor. Dent. Endod.* **2020**, *45*, e12.
40. Panov, V. Root canal treatment in elderly patients. *Varna Med. Forum* **2022**, *11*, 180–185.
41. Kuttler, Y. Aging changes in the teeth and their clinical importance. *J. Am. Dent. Assoc.* **1955**, *50*, 544–552.
42. Philippas, G.G. Influence of occlusal wear and age on formation of dentin and size of pulp chamber. *J. Dent. Res.* **1961**, *40*, 1186–1198.
43. Morse, D.R. Age-related changes of the dental pulp complex and their relationship to systemic aging. *Oral Surg. Oral Med. Oral Pathol.* **1991**, *72*, 721–745.
44. Kinney, J.H.; Nalla, R.K.; Pople, J.A.; Breunig, T.M.; Ritchie, R.O. Age-related transparent root dentin: mineral concentration, crystallite size, and mechanical properties. *Biomaterials* **2005**, *26*, 3363–3376.
45. Kaifu, Y.; Kasai, K.; Townsend, G.C.; Richards, L.C. Tooth wear and the "design" of the human dentition. *Am. J. Phys. Anthropol.* **2003**, *122*, 1–11.
46. Arola, D.; Reprogel, R.K. Tubule orientation and the fatigue strength of human dentin. *Biomaterials* **2005**, *26*, 4051–4060.
47. Peters, O.A.; Laib, A.; Göhring, T.N.; Barbakow, F. Changes in root canal geometry after preparation assessed by high-resolution computed tomography. *J. Endod.* **2000**, *26*, 1–6.
48. Michetti, J.; Maret, D.; Mallet, J.P.; Diemer, F. Validation of cone beam computed tomography as a tool to explore root canal anatomy. *J. Endod.* **2010**, *36*, 1187–1190.
49. Azimi, V. Comparison of dentinal wall thickness in the furcation area (danger zone) in the first and second mesiobuccal canals in the maxillary first and second molars using cone-beam computed tomography. *Eur. Endod. J.* **2020**, *5*, 81–85.
50. Yanık, D.; Nalbantoğlu, A.M. Dentin thickness at danger zone and canal morphology of maxillary molars. *Acta Stomatol. Croat.* **2022**, *56*, 50–60.
51. Bai, B.; Tang, Y.; Wu, Y.; Pei, F.; Zhu, Q.; Zhu, P.; Gu, Y. Ex vivo detection of mandibular incisors' root canal morphology using cone-beam computed tomography with 4 different voxel sizes and micro-computed tomography. *BMC Oral Health* **2023**, *23*, 656